Asia-Pacific Journal of Science and Technology: Volume: 28. Issue: 02. Article ID.: APST-28-02-04. Research Article

APST

Asia-Pacific Journal of Science and Technology

https://www.tci-thaijo.org/index.php/APST/index

Published by the Research and Technology Transfer Affairs Division,
Khon Kaen University, Thailand

# Durability performance of geopolymer mortar containing high calcium fly ash and low-grade waste clay

Sreedevi Lekshmi[1,*], J Sudhakumar[1] and Sneha Thomas[2]

[1]Department of Civil Engineering, National Institute of Technology Calicut, Kerala, India
[2]APJ Abdul Kalam Technological University, Trivandrum, Kerala, India
[*]Corresponding author: sreedevilekshminair@gmail.com

Received 7 August 2021
Revised 25 November 2021
Accepted 8 January 2022

**Abstract**

The primary objective of this research work was to investigate the durability performance of class C fly ash-based geopolymer mortar containing locally available waste clay as source material. The experiments were conducted based on the 20 design trials obtained using response surface methodology (RSM). For this study, the waste clay was collected from few sources of India. The clays in their raw state and after thermal treatment was taken for the investigation. The analysis for optimization was based on parameters such as dry density, compressive strength and water absorption. The optimum combination of clay (with and without thermal treatment) in class C fly ash-based geopolymer mortar was obtained with molarity of NaOH at 7M and 9M with a temperature of curing at 56°C and with clay content of 20%. Durability performance of optimum mix in terms of water absorption, sorptivity, acid attack resistance, sulfate attack resistance, abrasion resistance, drying shrinkage and impact resistance were studied. Thermally treated clay-based specimens exhibited better durability characteristics than specimens with clay in the raw state.

**Keywords:** Dry density, Compressive strength, Water absorption, Sorptivity, Abrasion resistance, Molarity, Fly ash, Clay

## 1. Introduction

Cement is regarded as an inevitable part of the construction industry as it acts as an excellent binder, and its demand will continue to expand significantly in the coming decades. But its production process is energy-intensive and contributes towards global warming due to the emission of carbon dioxide gas. Previous studies reveal that the production of one ton of cement produces approximately one ton of $CO_2$ gas to the atmosphere, which is highly deleterious to the life of our planet. The other environmental impacts associated with the cement production include noise pollution resulting from operating machinery and the release of fine dust and other gases into the atmosphere. Therefore, in 1978, Davidovits developed the geopolymer binder as an alternate binder that used industrial wastes instead of cement [1]. There are studies that reveal that the development of geopolymer binder reduces the $CO_2$ emission by 80% with 60% less consumption of energy [2-3].

Geopolymer binder has two parts, the source material and an alkaline medium. The source materials are activated by the alkaline medium. Commonly used source materials are aluminosilicate rich industrial wastes (examples: fly ash, ground granulated blast furnace slag) and agricultural wastes (examples: rice husk ash, sugarcane bagasse ash) [4-11]. The peculiar property of a waste material to be used as source material in geopolymers is its rich aluminates and silicates content. The alkaline mediums commonly used are a combination of sodium hydroxide and sodium silicate or potassium hydroxide and potassium silicate. Developing geopolymers by using two source materials (examples: fly ash and ground granulated blast furnace slag, fly ash and rice husk ash, fly ash and red mud, etc.) are known as binary geopolymer binder [10]. Geopolymer has its advantages such as sustainable construction, longer life span, reduction in $CO_2$ emission and hence reduces global warming, effective utilization of industrial or agricultural wastes, economic and maintenance required is less [12].

Clays have surplus aluminosilicate content, making them an ideal source material from waste in geopolymer binders. Priyadharshini et al [13] studied the effect of using excavated soil waste with different plasticity as fine aggregate in geopolymer mortar (GPM). The properties of GPM were affected by the molarity of NaOH. The compressive strength improved from 78-128% in plastic soil-based GPM. Water absorption and drying shrinkage increased with an increase in the molarity of NaOH. It was observed that the strength and shrinkage properties were influenced by the type of clay used [13].

According to Lekshmi et al [14], GPM specimens containing class C fly ash and flood soil waste were evaluated for engineering and durability performance. In the study, the test results were compared with the GPM specimens containing lime treated flood soil waste. It was observed that the engineering performance in terms of compressive strength, split tensile and flexural strength were improved by 21.44%, 16.03% and 3.04%, respectively, after lime treatment. The durability properties in terms of water absorption, sorptivity, impact resistance, drying shrinkage and abrasion resistance were improved by 46.36 %, 41.52%, 11.11%, 53.97 and 33.03%, respectively, after lime treatment. The resistance towards acid and sulfate attack improved by 8.59% and 20.8%, respectively [14].

In a study based on synthesis of geopolymer using Nigerian clay was used in developing GPM in its raw state and after calcining. The study revealed that calcined clay up to 25% can be utilized in developing geopolymers. Also, the incorporation of calcined clay in geopolymers accelerated the dissolution of fly ash in alkaline medium. The improvement in compressive strength with the addition of calcined clay is related to the enhanced reactivity of fly ash and calcined clay [15].

In the study performed by Zreig et al [16] to evaluate the influence of thermal treatment on the properties of clayey soils, it was reported that a significant improvement in physical properties in terms of Atterberg limit, optimum water content, unconfined compressive strength, swelling pressure and dry density were observed at 400°C.

Even though there are studies that reported the use of clay as source material and fine aggregate in geopolymer mortar, there is a need for a structured and organized investigation on its engineering and durability properties. Also, the detailed research is essential for using treated clay as a source material in geopolymers. The present study evaluates the durability characteristics of binary GPM containing high calcium fly ash with different types of waste clay in the raw state and after thermal treatment. In this study, two varieties of clay with different plasticity were used. The geopolymer mortars were synthesized based on parameters such as molarity of NaOH, temperature of oven curing and clay content. The factor sodium silicate to sodium hydroxide ratio was chosen as one. It is expected from the test results that the geopolymer binder obtained by integrating waste clay with class C fly ash can be used for developing repair material for structural elements, non-load bearing elements, wall panels, insulating material, prefabricated building blocks, as fillers in floors and roofs and in lightweight construction.

## 2. Materials and methods

### *2.1 Materials*

The primary source material used for the investigation was Class C fly ash according to American Society for Testing and Materials (ASTM) C 618, collected from Neyveli thermal power station [17]. Waste clay excavated during construction (Figure 1A) with grey color (GC) and waste clay removed from paddy field (Figure 1B) with brown color (BC) collected from Calicut region was used for the investigation in replacing the fly ash. Thermally treated excavated grey clay (TGC) and that of paddy brown clay (TBC) were developed by placing clays in a muffle furnace at an elevated temperature ranging between 500-750°C (Figure 1C and 1D). The optimum temperature for thermal treatment of clays were obtained by performing the trial-and-error method. The optimum temperature for the thermal treatment of GC and BC was obtained at 600°C and 550°C, respectively. The chemical and physical properties of fly ash and clays are shown in Tables 1 and 2, respectively. The pozzolanic activity (PAI) of thermally treated clay was observed to be higher than that of clay in its raw state (Table 2). This is due to the dehydroxylation during the thermal treatment resulting in the destruction of the crystalline structure and development of an amorphous structure with an increased reactivity [18]. The pH values for GC and BC are different and the change in pH after thermal treatment is attributed to the process of rehydroxylation [19]. The liquid limit for GC, BC, TGC and TBC was 65.55%, 50.19%, 39.16% and 39.60%, respectively. Plastic limit for GC, BC, TGC and TBC was obtained as 32.50%, 32.30%, 26.50% and 21.41%, respectively. Shrinkage limit was obtained as 31.73%, 30.27%, 27.45% and 20.90%, respectively for GC, BC, TGC and TBC. The decrease in in the Atterberg limit values of GC and BC after thermal treatment is attributed to the change in the size of the clay particles, surface charge and surface area of the clay particles, dehydration and decomposition of the clay particles, change in minerology and microstructure of the clay particles and change in interparticle contact area leading to the removal of diffuse double layer upon exposing to the elevated temperature [20].

The silica-rich river sand was used as fine aggregate (pass through 4.75 mm Indian Standard (IS) sieve). The specific gravity and fineness modulus of the river sand used was 2.67 and 3.39, respectively. The alkaline solution required for executing the design trials by experiment was synthesized by blending the appropriate amount of sodium silicate ($Na_2SiO_3$) and sodium hydroxide solution (NaOH). $Na_2SiO_3$ solution was observed as highly viscous and gelatinous. The reaction of NaOH is exothermic with water. Hence NaOH solution was prepared by dissolving NaOH pellets a day before casting, in distilled water. The mixing of NaOH and $Na_2SiO_3$ was performed one hour before the cast. From the previous literature, the sodium silicate to sodium hydroxide ratio (S/N) was fixed as one [4,13].

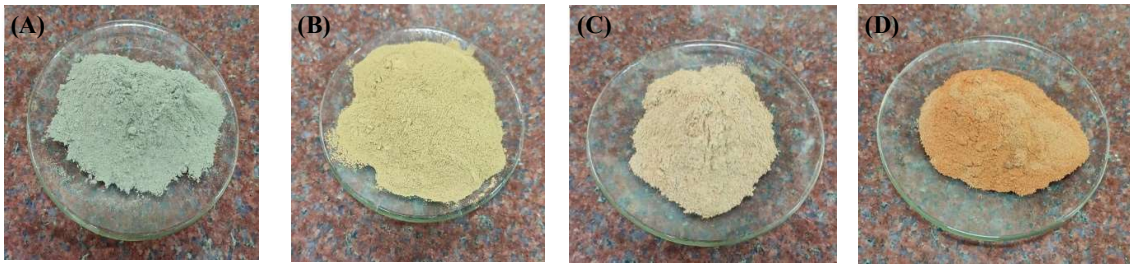


**Figure 1** Different clays used for investigation (A) GC (B) BC (C) TGC and (D) TBC.

**Table 1** Chemical composition of fly ash and clays (XRF analysis).

| Chemical composition (%) | $SiO_2$ | $Al_2O_3$ | $Fe_2O_3$ | $K_2O$ | CaO | $Na_2O$ | $SO_3$ | MgO | $P_2O_5$ |
|---|---|---|---|---|---|---|---|---|---|
| Class C fly ash | 43.98 | 23.55 | 4.93 | 1.84 | 21.65 | 0.57 | 1.44 | 1.81 | - |
| GC | 31.05 | 27.85 | 5.02 | 0.85 | 1.24 | 0.94 | 0.25 | 2.27 | 0.21 |
| BC | 32.62 | 27.94 | 7.77 | 0.43 | 0.42 | 0.36 | 0.20 | 0.97 | 0.26 |
| TGC | 48.65 | 31.65 | 4.95 | 0.88 | 1.23 | 1.04 | 0.13 | 2.38 | 0.22 |
| TBC | 45.51 | 29.85 | 7.81 | 0.42 | 0.39 | 0.32 | 0.11 | 0.99 | 0.26 |

**Table 2** Physical characteristics of fly ash and clays.

| Physical properties | Fly ash | GC | BC | TGC | TBC |
|---|---|---|---|---|---|
| Colour | Dark grey | Grey | Rust brown | Orangish brown | Brick red |
| Specific gravity | 2.30 | 2.43 | 2.13 | 2.33 | 2.17 |
| PAI (%) (ASTM C 311) [21] | 81.34 | 77.49 | 79.48 | 82.14 | 80.07 |
| pH | 11.00 | 7.13 | 7.38 | 11.20 | 9.80 |

*2.2 Mix proportioning*

The central composite design (CCD) is used in generating a set of twenty design trials. For designing trials, a set of three parameters and their range was taken from the previous literature. These parameters include the molarity of NaOH solution (6-10 M), the temperature of curing (50-80°C) and the percentage of clay (0-100%). All the design trials were conducted experimentally based on the parameters of each trial to obtain the optimum composition. The optimization was performed based on the compressive strength (CS), dry density and water absorption. Durability studies were conducted on the various optimum combinations obtained. A dissolution time of 24 h was permitted for all specimens before oven curing. Specimens were cured at a specified temperature in a hot air oven for each trial for 24 h. Design trials from RSM and the corresponding mix proportions in $kg/m^3$ are reported in Table 3.

**Table 3** Design trials based on RSM and corresponding mix proportion in kg/m$^3$.

| Trial No. | Molarity of NaOH (M) | Temperature of curing (°C) | Percentage of clay (%) | Fly ash (kg/m$^3$) | Clay (kg/m$^3$) |
|---|---|---|---|---|---|
| 1 | 8 | 80 | 50 | 665 | 665 |
| 2 | 9 | 74 | 80 | 266 | 1064 |
| 3 | 7 | 74 | 20 | 1064 | 266 |
| 4 | 7 | 74 | 80 | 266 | 1064 |
| 5 | 9 | 74 | 20 | 1064 | 266 |
| 6 | 8 | 65 | 50 | 665 | 665 |
| 7 | 8 | 65 | 50 | 665 | 665 |
| 8 | 8 | 65 | 100 | - | 1330 |
| 9 | 8 | 65 | 50 | 665 | 665 |
| 10 | 8 | 65 | 50 | 665 | 665 |
| 11 | 8 | 65 | 50 | 665 | 665 |
| 12 | 8 | 65 | 50 | 665 | 665 |
| 13 | 8 | 65 | 0 | 1330 | - |
| 14 | 6 | 65 | 50 | 665 | 665 |
| 15 | 10 | 65 | 50 | 665 | 665 |
| 16 | 9 | 56 | 20 | 1064 | 266 |
| 17 | 7 | 56 | 20 | 1064 | 266 |
| 18 | 9 | 56 | 80 | 266 | 1064 |
| 19 | 7 | 56 | 80 | 266 | 1064 |
| 20 | 8 | 50 | 50 | 665 | 655 |

Note: River sand (kg/m$^3$) = 1330.

### *2.3 Experimental program*

The mixes were prepared based on the trials reported in Table 4. The workability of the fresh GPM for each design trials was carried out by the flow table test. For performing the optimization study, dry density, CS and water absorption for each trial were investigated. Durability performances of the optimum mix based on the water absorption, sorptivity, resistance towards chemical attack, abrasion resistance, drying shrinkage and impact resistance were studied.

The workability of fresh GPM in the fresh state for each trial mix was studied using the flow table test as per ASTM C1437-15 [22]. In all the cases, the liquid alkaline to the binder ratio was taken in such a way to keep the workability constant as 110±5%. Three flow readings were taken and averaged to maintain accuracy.

The CS of GPM specimens were determined based on ASTM C109 [23]. Six number of 5 cm cube specimens were taken for each mix. The dry density was determined by keeping the cube specimens in oven at 110±5°C for 24 h and then cooled to room temperature.

Water absorption (WA) of GPM specimens were determined based on ASTM C 1403-15 [24]. An average of three 5 cm cube specimens were taken for WA. The sorptivity was evaluated based on ASTM C1585-13 [25]. Cylindrical specimens of 100 mm diameter and 50 mm height were used. The average of the slope of the cumulative volume of water absorption versus square root of time interval graph of two specimens were taken as sorptivity. The acid and sulfate attack resistance of the GPM were determined based on ASTM C1898-20 and ASTM C 267-20, respectively [26,27]. IS 15658: 2006 was used for testing the resistance towards abrasion [28]. Four cube specimens of size 7 cm were taken for the study. Drying shrinkage was tested on prisms of size 160 × 40 × 40 mm as per ASTM C157 [29]. Three specimens were taken for the study. The impact resistance of GPM was studied by the weight drop method based on ACI 544.2R-89 [30]. The average of three cylindrical specimens of size 150 mm diameter and 50 mm height was taken.

## 3. Results and discussion

### *3.1 Characterization of clay*

X-ray diffraction (XRD) results (Figure 2A) of GC and BC revealed the presence of its various minerals. The main minerals present in GC were Kaolinite (K), Quartz (Q) and Calcite (C), and the main minerals present in BC were Illite (It), Q and C. Kaolinite is a clay mineral that consist of a single silica tetrahedral sheet and single alumina octahedral sheet. Quartz is the primary source of silica in clay. Calcite is the natural form of calcium carbonate present in the clay. Illite is a clay mineral that is of non-expanding type.

In FTIR analysis of both clays, the band at 1050 cm$^{-1}$ represents the stretching of Si-O bond (Figure 2B). In the TGA analysis of GC and BC, the samples were heated from room temperature to 200°C, as shown in Figure 2C. A significant reduction in the weight is observed till 80°C for both GC and BC, which is attributed to the loss of physical impurities and absorbed water. The scanning electron microscope (SEM) images (Figure 2D and 2E) also revealed the presence of kaolinite in GC and illite in BC. In SEM images, the dark region represents Quartz, the very finely hairy structures, Illite, the fine sheet-like structures, K, and the plate-like structures, Calcite. The microstructural characterization of thermally treated GC and BC are given in Figure 3.

From Table 1, it is evident that the $SiO_2$ content increased from 31.05% to 48.65%, for GC and 32.62% to 45.51% for BC after thermal treatment. Again, $Al_2O_3$ content increased from 27.85% to 31.65% for GC and 27.94% to 29.85% for BC after thermal treatment. The XRD pattern of TGC and TBC revealed the presence of halo peaks at 20º 2θ and 30º 2θ (Figure 3A). It is due to the amorphous silica formed by the thermal treatment of GC and BC containing crystalline silica in the form of quartz [15]. Also, the considerable increase in oxides of silica and alumina is due to the decrease in the loss on ignition content after thermal treatment [31].

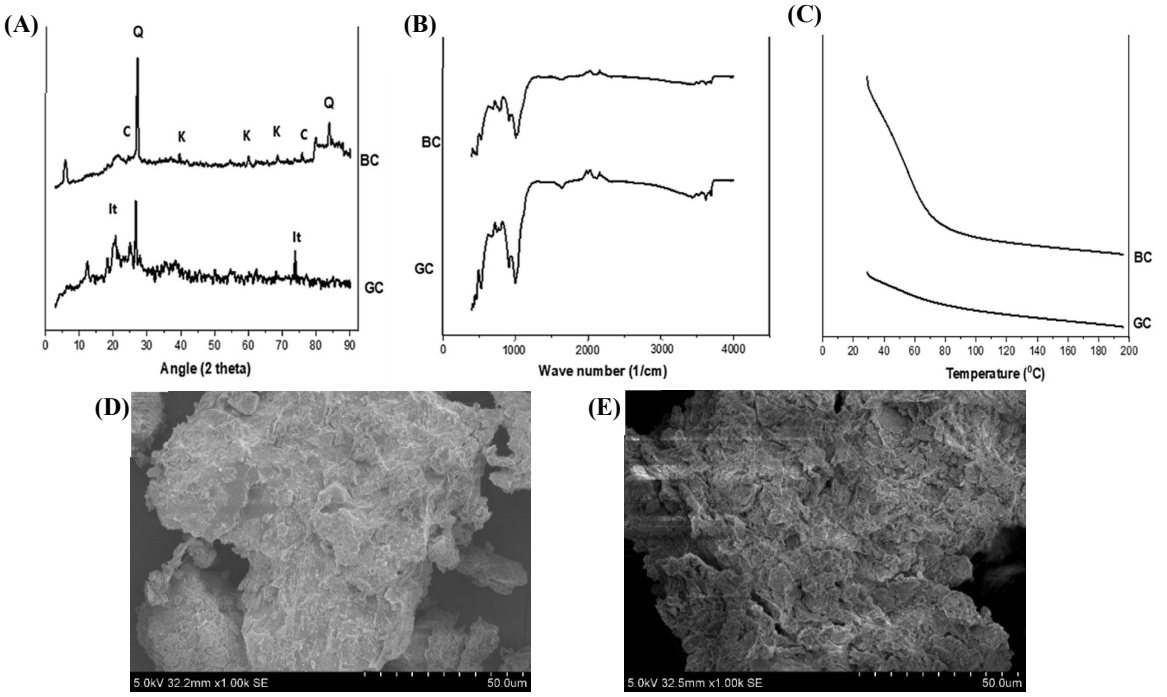


**Figure 2** (A) XRD of GC and BC (B) FTIR of GC and BC (C) TGA analysis of GC and BC (D) SEM of GC (E) SEM of BC.

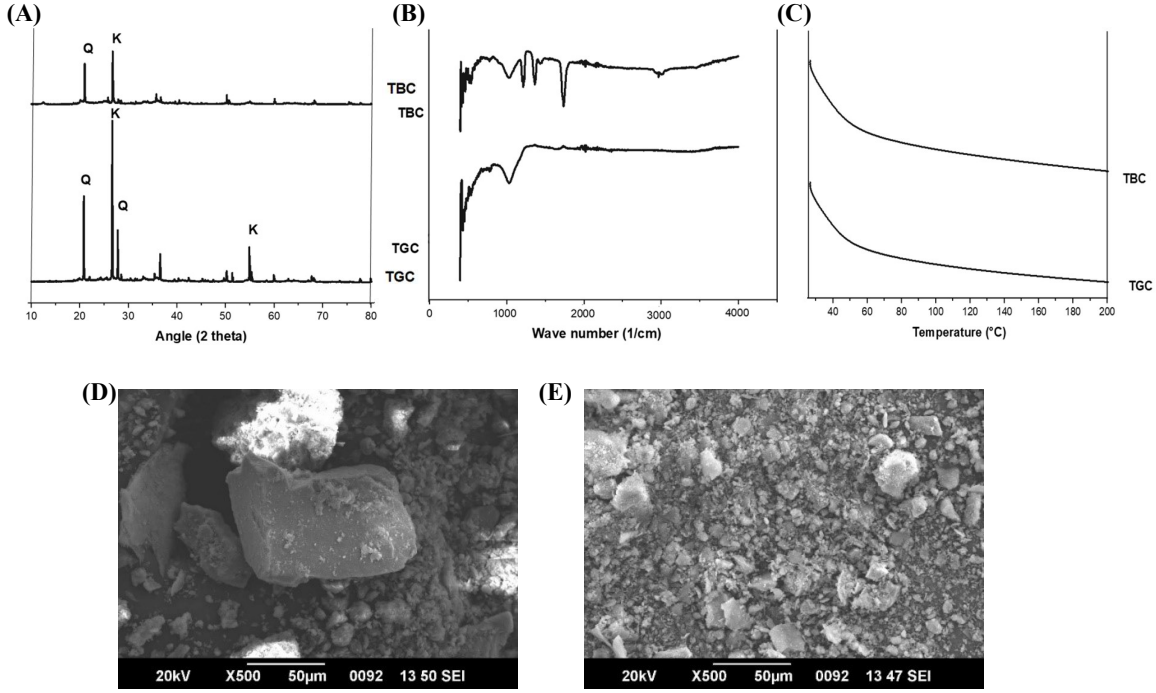


**Figure 3** (A) XRD of TGC and TBC (B) FTIR of TGC and TBC (C) TGA analysis of TGC and TBC (D) SEM of TGC (E) SEM of TBC.

*3.2 Workability of GPM*

It is evident from table 4 that the ratio of alkaline solution to the combination of class C fly ash and clay (untreated and thermally treated) increased with the molarity of NaOH solution and clay content. For thermally treated clays, the demand for alkaline solution decreased to meet the required workability when compared with the clays in the raw state. This is due to the reduction in the internal surface area of the clay minerals as a result of de-hydroxylation [32]. Using the Scherrer equation, the internal surface area of GC, BC, TGC, and TBC were calculated in the present study. With the same equation, the crystalline size of GC, BC, TGC, and TBC were obtained as 162.44 nm, 129.86 nm, 976 nm, and 751.09 nm, respectively. The surface area is inversely related to the crystalline size. It implies that the surface area of the clay particles reduced with the thermal treatment.

**Table 4** Liquid alkaline to binder ratio for design trials for untreated and thermally treated clay.

| Trial No. | Liquid alkaline to binder ratio | | | |
|---|---|---|---|---|
| | GC | BC | TGC | TBC |
| 1 | 1.20 | 1.20 | 0.95 | 0.92 |
| 2 | 1.25 | 1.20 | 0.95 | 0.92 |
| 3 | 1.00 | 1.00 | 0.80 | 0.80 |
| 4 | 1.50 | 1.00 | 0.98 | 0.80 |
| 5 | 1.00 | 1.20 | 0.80 | 0.92 |
| 6 | 1.20 | 1.20 | 0.92 | 0.92 |
| 7 | 1.20 | 1.20 | 0.92 | 0.92 |
| 8 | 1.28 | 1.30 | 0.92 | 0.92 |
| 9 | 1.00 | 1.20 | 0.80 | 0.92 |
| 10 | 1.00 | 1.20 | 0.80 | 0.92 |
| 11 | 1.00 | 1.20 | 0.80 | 0.92 |
| 12 | 1.00 | 1.20 | 0.80 | 0.92 |
| 13 | 0.90 | 0.90 | 0.85 | 0.85 |
| 14 | 1.00 | 1.20 | 0.80 | 0.92 |
| 15 | 1.20 | 1.25 | 0.92 | 0.92 |
| 16 | 1.00 | 1.20 | 0.80 | 0.92 |
| 17 | 1.00 | 1.00 | 0.80 | 0.80 |
| 18 | 1.00 | 1.20 | 0.80 | 0.92 |
| 19 | 1.00 | 1.00 | 0.80 | 0.80 |
| 20 | 1.00 | 1.20 | 0.80 | 0.92 |

*3.3 Optimization of clay in class C fly ash-based GPM*

To obtain the optimum combination of parameters in terms of the molarity of NaOH, the temperature of curing and the percentage of clay and for synthesizing and studying the durability performance of GPM specimens, CCD of RSM was used. The study for optimization was based on the combination of the above-said parameters that gave maximum CS and dry density with minimum water absorption.

*3.3.1 Dry density*

The variation in dry density with respect to temperature of curing and molarity of NaOH was observed to be linear for GC, BC, TGC and TBC in class C fly ash and is shown in Figure 4. At a constant S/N ratio of 1, the molarity of NaOH and the curing temperature has a significant effect on the dry density. When the temperature of curing was increased from 50- 80°C, the dry density decreased linearly after attaining an optimum temperature. Also, with the increase in molarity of NaOH from 6 M to 10 M, the dry density increased linearly. This is related to the enhancement in geopolymerization process when the molarity was increased and by which the activation products get filled in the void or pore space in the mortar specimens, as supported by Priyadharshini et al [13]. It is also reported that with an increase in the plasticity of clay, the dry density reduces, which is further related to the reduction in the bulk density of highly plastic/cohesive clay due to the increased clay content. The dry density also decreased as the percentage of clay replacement increased from 0% to 100% [13].

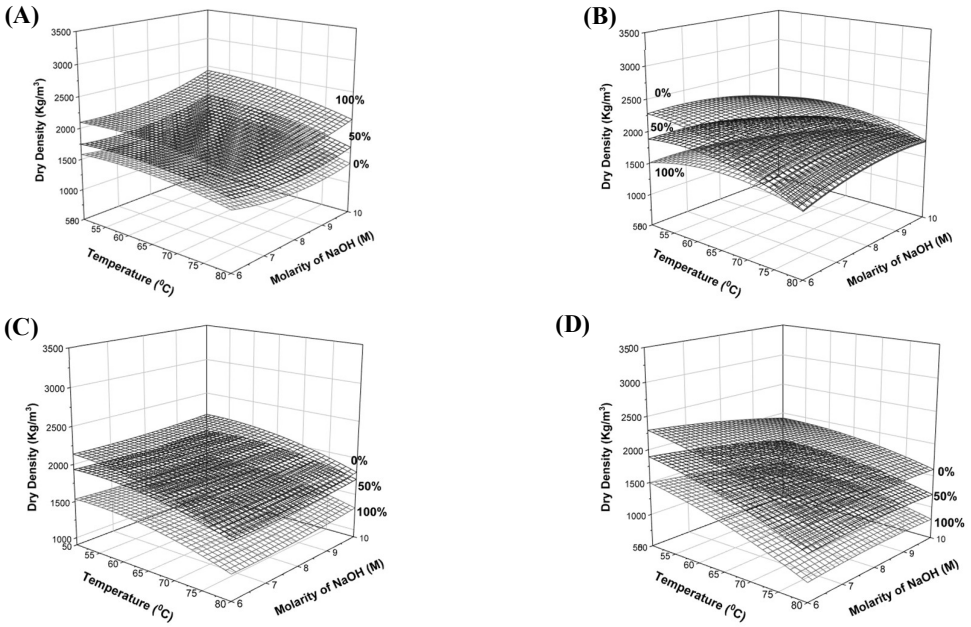


**Figure 4** Dry density for GPM specimens with (A) GC, (B) BC (C) TGC and (D) TBC.

*3.3.2 Compressive strength*

The variation of CS with an increase in the curing temperature (50-80°C) and the molarity of NaOH (6M to 10M) at different percentage of the clay content (0-100%) is presented in Figure 5. It was observed that, in all the cases, the CS increased to an optimum value of the temperature of curing along with the molarity of NaOH and then decreased. The strength attainment was influenced by factors such as dissolution of aluminosilicates present in fly ash and clay in the alkaline medium, specific surface area of clays and plasticity of clays used [33-35]. The optimum composition was observed to be at a molarity of 7M, 56°C of temperature and at 20% clay for GC and TGC. For BC and TBC, the optimum composition was at 9M, 56°C and 20% clay. TGC and TBC exhibited 80.18% and 58.59% increase in the CS than that the raw state. This is attributed to the improvement in the pozzolanic activity of both clays after the thermal treatment, which enhanced the CS. Also, the endothermic reactions that happened during the thermal treatment of clay resulted in the removal of the adsorbed and bound water in the clay along with the dehydroxylation of the clay structure. Hence it is concluded that the amorphous nature of the thermally treated clay made it reactive in the alkaline medium which further resulted in an increase in the CS [32].

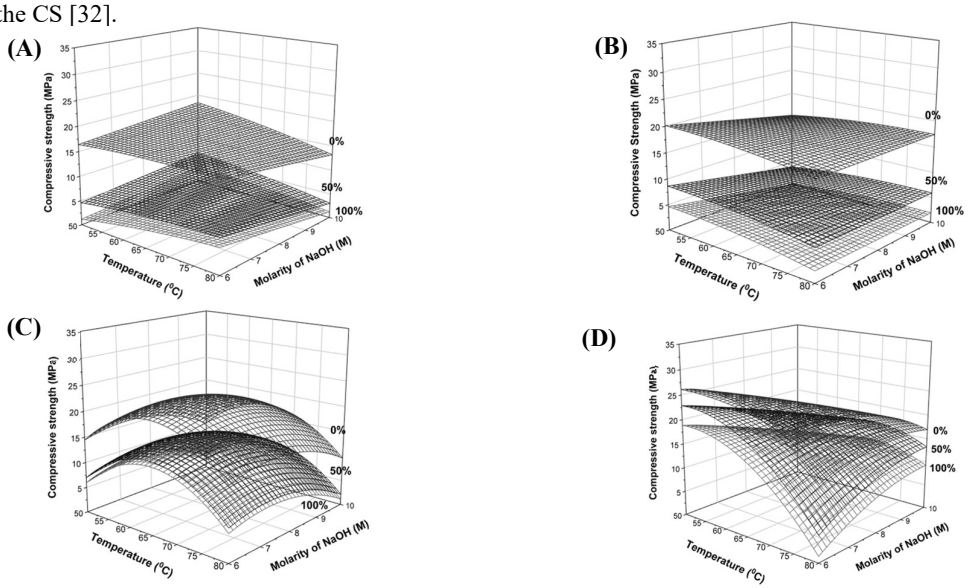


**Figure 5** Compressive strength of GPM specimens with (A) GC, (B) BC, (C) TGC and (D) TBC.

*3.3.3 Water absorption*

The water absorption decreased linearly with the molarity of NaOH for S/N of 1 at all percentages of clay (Figure 6). Water absorption in low plastic soil was least when compared with the soils of medium and high plasticity, and for low plastic soil, the former is 18-20% [34]. When the clay minerals attain contact with the strong base i.e., the NaOH solution, the complete ionization of the ions takes place, which further reacts with the Si and Al species present in the minerals. In the case of kaolinite and halloysite clay minerals, the 1:1 layer structure is highly susceptible to the attack of NaOH in which a greater amount of Al is removed than Si. The predominant 2:3-layer structure in montmorillonite and illite, much amount of Al is removed by the attack of NaOH. The stability of the clay layers is affected by the presence of NaOH. The binding of soil particles is hindered by the displacement of $Na^+$ ions. The clay double-layer thickens with alkali contact due to the larger radius of $Na^+$ ions. The further swelling and dispersing of the clay structure occurs due to the inter-particle repulsion due to an increase in the negative charge of the soil with the addition of high pH solution (i.e., NaOH) [36]. The optimum combination based on the CS, dry density and water absorption is reported in Table 5.

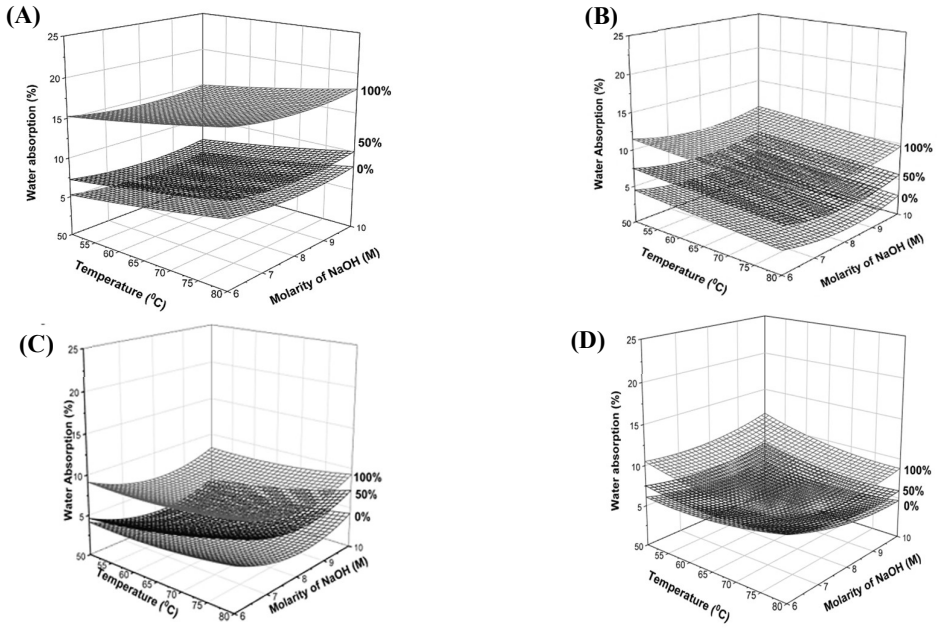


**Figure 6** Water absorption for GPM specimens with (A) GC, (B) BC, (C) TGC and (D) TBC.

**Table 5** Compressive strength, dry density and water absorption of optimum combinations.

| Optimum mix | Class C fly ash with waste clay | | | | | |
|---|---|---|---|---|---|---|
| | Raw clay | | | Thermally treated clay | | |
| | Compressive strength (MPa) | Dry density ($Kg/m^3$) | Water absorption (%) | Compressive strength (MPa) | Dry density ($Kg/m^3$) | Water absorption (%) |
| GC | 9.99 | 1998 | 3.17 | 18.00 | 2000 | 2.56 |
| BC | 11.98 | 2010 | 3.78 | 19.00 | 2105 | 3.18 |

*3.4 Durability performance*

*3.4.1 Water absorption and sorptivity*

Table 6 shows the water absorption recordings for the various optimum combinations. The thermally treated clay incorporated class C fly ash-based GPM specimens exhibited lower water absorption. The calcined clay incorporated class C fly ash-based GPM specimens exhibited lower sorptivity than raw clay-based specimens. Due to the increase in the pozzolanicity of calcined clays, the capillary pore size reduced, leading to the densification of the microstructure. This is further attributed to the coexistence of aluminosilicate and calcium silicate hydrate (CSH) gel and hence penetration of water decreased [37].

**Table 6** Water absorption and sorptivity of optimum combinations of GPM.

| Mix proportion | Water absorption (%) | Sorptivity (cm/min$^{1/2}$) × 10$^{-3}$ |
|---|---|---|
| GC-GPM | 3.17 | 2.96 |
| BC-GPM | 3.78 | 2.51 |
| TGC-GPM | 2.56 | 1.73 |
| TBC-GPM | 3.18 | 2.21 |

(GC-GPM- excavated grey clay-based GPM, BC-Paddy brown clay-based GPM, TGC- thermally treated GC based GPM, TBC- thermally treated BC based GPM).

*3.4.2 Resistance towards chemical attack (acid attack and sulfate attack)*

The change in flexural strength and change in weight is shown in Table 7. GPM specimens with calcined clay showed better resistance towards acid attack. The breakage in the aluminosilicate bond is attributed to the reduction in strength of GPM after exposure to sulfuric acid. The weight loss and change in the compressive strength were observed to study the influence of sodium sulfate on GPM specimens and are reported in table 8. Sulfate attack resistance was more for GPM specimens with thermally treated clay [38]. The geopolymer mortar specimens containing thermally treated clay exhibited better resistance towards the acid attack with surface damage, mass loss and deterioration of compressive strength. This is because, the micro-particles of the thermally treated clay fill up the pore space resulting in the formation of significant quantity of hydrates which further leads to the development of a dense microstructure. Thus, the expanding and dissolving effect of the thermally treated clay incorporated geopolymer mortar specimens in the acid medium gets mitigated [39]. Sulfate attack is related to the reaction of sulfate ions with calcium hydroxide and calcium aluminate hydrate that leads to the development of gypsum and ettringite. The formation of gypsum is responsible for the softening, mass loss and hence strength deterioration of the specimens. The mass loss is due to the leaching of CSH gel in the matrix [38]. The flexural strength of samples before exposing to acid solution for GC, BC, TGC and TBC are 5.91 MPa, 6.68 MPa, 8.33 MPa, 7.97 MPa, respectively. The compressive strength of GPM cube specimens before exposing to sulfate solution for GC, BC, TGC and TBC are 9.99 MPa, 11.98 MPa, 14.21 MPa and 19.45 MPa, respectively.

**Table 7** Acid and sulfate attack resistance of GPM specimens.

| Mixture | Acid ttack | | Sulfate attack | |
|---|---|---|---|---|
| | Weight loss (%) | Flexural strength loss (%) | Weight loss (%) | Compressive strength (loss %) |
| GC-GPM | 3.46 | 34.92 | 9.27 | 35.28 |
| BC-GPM | 2.97 | 31.37 | 5.35 | 23.75 |
| TGC-GPM | 2.23 | 17.65 | 3.76 | 15.50 |
| TBC-GPM | 2.06 | 10.67 | 3.48 | 12.92 |

*3.4.3 Abrasion resistance*

The abrasion resistance of the GPM specimens presented in Table 8 indicates that thermally treated clay-based GPM specimens exhibited better abrasion resistance in terms of the volume change which is attributed to the development of a dense microstructure [40].

**Table 8** Abrasion resistance of GPM.

| Mix proportion | Abrasion resistance (cm$^3$) |
|---|---|
| GC-GPM | 14.20 |
| BC-GPM | 13.67 |
| TGC-GPM | 9.54 |
| TBC-GPM | 10.23 |

*3.4.4 Drying shrinkage*

For all the cases, the shrinkage decreased with an increase in the molarity of NaOH and the temperature of curing at a constant S/N ratio of one. The increase in curing temperature helped in the polymerization and resulted in the formation of a dense-structure. The shrinkage was observed to be reduced irrespective of the type of clay used after thermal treatment. With an increase in the percentage replacement of clay from 0% to 100%, the shrinkage increased. The drying shrinkage of GPM specimens of optimum combination is shown in Figure 7. TGC and TBC showed lower drying shrinkage.

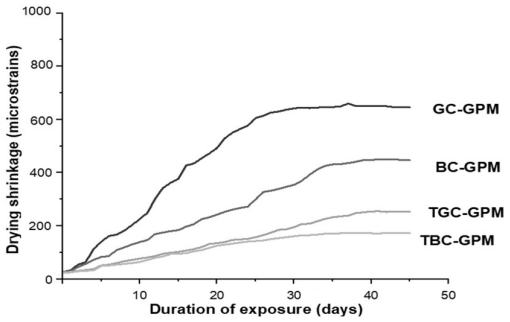


**Figure 7** Drying shrinkage of GPM specimens of optimum combination.

*3.4.5 Impact resistance*

The regions of the hurricane, railway sleepers, harbors, etc., are the circumstances where the impact resistance of the structures or structural elements is highly significant. Calcined clay-based GPM specimens showed better resistance towards impact due to the coexistence of CSH gel and aluminosilicate gel and contributes towards the development of a dense microstructure (Figure 8) [5]. The impact energy of GPM specimens is reported in Table 9.

**Table 9** Impact energy of GPM specimens.

| Mix proportion | 1st crack blows | Failure crack blows | Impact energy (nm) |
|---|---|---|---|
| GC-GPM | 31 | 39 | 699.37 |
| BC-GPM | 30 | 35 | 627.64 |
| TGC-GPM | 44 | 51 | 914.57 |
| TBC-GPM | 42 | 49 | 878.70 |

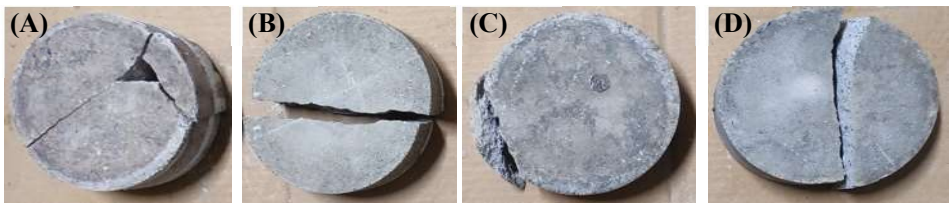


**Figure 8** Specimens after impact testing using dropping weight method; (A) GC, (B) BC, (C) TGC, and (D) TBC.

*3.5 Discussion*

The present study focusses on synthesizing geopolymer mortar using high calcium fly ash and waste clays by studying its mechanical and durability characteristics. The various parameters considered for developing the geopolymer based on RSM was molarity of NaOH, temperature of oven curing and percentage of clay. The results of the current study shows that the optimum mix was the mix proportion that exhibited maximum dry density and compressive strength with lower water absorption. During optimization, it was observed that the dry density, CS and water absorption improved with the thermal treatment of clays. The deterioration of the layered structure of the clay after thermal treatment resulted in the accelerated dissolution of alumina and silica of clays in the alkaline medium [34]. Studies reveal that the sodium silicate and sodium hydroxide exhibited better dissolution of aluminosilicate species than the potassium based alkaline solutions [41]. Molarity of NaOH was observed as a significant parameter that affected the dry density, compressive strength and water absorption of geopolymer mortar samples with clay. Dry density and CS increased with molarity of NaOH up to an optimum value and then decreased. But water absorption decreased up to an optimal level with elevation in NaOH molarity. This was in agreement with the attributes by Gorhan and Kurklu as dissolution of fly ash is higher at higher molarities of NaOH, and the polycondensation is restricted at higher molarities [33]. As per the study of Dietel, the CS of GPM was influenced by the specific surface area of the clay particles used as source material [34]. According to the investigations of Priyadharshini et al [13], the effect of temperature remains unnoticed at higher molarities of NaOH solution for non-plastic soils [13]. Ogundiran observed the compressive strength increased with the NaOH concentration which was attributed to the polycondensation of alumina and silica species after its dissolution in the strong alkaline medium [35]. Compressive strength and dry density increased with an increase in curing temperature from 50-80°C up to an optimum value of 74°C. It was due to the enhancement in the

geopolymerization process at elevated temperatures resulting in the development of a dense and stiff matrix [13]. Again, with the increase in clay content from 0% to 100%, CS and dry density decreased and water absorption increased. It is due to the increase in pores and voids in the GPM and agrees with the observations of Priyadharshini et al [13].

The durability performance in terms of water absorption, sorptivity, abrasion resistance, drying shrinkage, impact resistance, acid and sulfate attack resistance also improved with the thermal treatment of clays. The reduction in water absorption and sorptivity with the thermal treatment of clay is ascribed to the existence of CSH gel phase in conjunction with the aluminosilicate gel [5,6]. The enhancement in acid and sulfate attack resistance for TGC and TBC based GPM is attributed to the reduction in the development of pores in specimens that results in high rate of depletion of aluminosilicate gel from the matrix [5,6,42,43].

In a study by Lekshmi et al [14], it was observed that the engineering and durability properties of GPM specimens containing class C fly ash and silicious flood soil waste, improved with the lime treatment of flood soil waste. It was due to the filling up of void space with CSH gel in lime treated GPM specimens. In this study, the abrasion resistance and impact resistance of flood soil waste-based GPM improved by 33.03% and 11.11%, respectively, after lime treatment. The water absorption and sorptivity were observed to be reduced after lime treatment by 46.31% and 41.50%, respectively [14]. In a study by Priyadharshini et al [13], the drying shrinkage was obtained in the range 500 to 1200 microstrains for medium and plastic clay-based specimens and 700 to 1625 microstrains for high plastic clay-based specimens [13]. The experiments performed by Saranya et al. revealed that the ground granulated blast furnace slag (GGBS) dolomite based GPM exhibits better engineering and durability properties than ordinary Portland cement (OPC) due to the coexistence of aluminosilicate and CSH gel in GPM specimens. The durability performances in terms of water absorption, porosity, sorptivity and resistance to acid and sulfate attack were studied [44]. The reduction in sorptivity of TGC and TBC based GPM specimens in the present study is attributed to the densification of the microstructure of the specimens as a result of reduced pore size and was supported by the observations of Kasim et al [45].

The study can be further extended by treating the clay with various methods that enhance its mechanical and durability characteristics. The treatment methods include incorporating the calcium and silica-based materials such as lime, ground granulated blast furnace slag, dolomite, rice husk ash, palm oil fuel ash, sugar cane bagasse ash, class F fly ash, etc. Also, by incorporating various fibers in clay as part of treating the clay, the performance of geopolymer matrix can be improved.

## 4. Conclusion

From the test results of present study, a decrease in compressive strength was observed with an increase in clay content. The optimum molarity of NaOH for GC and BC was 7M and 9M, respectively, with curing temperature at 56°C. With the increase in molarity of NaOH and clay content, more amount of liquid alkaline solution was required to maintain the standard workability. With an increase in NaOH molarity, the solution's viscosity increased, and hence water demand increased. For thermally treated clay-based mortar mix, a significant reduction in water demand was observed to meet the required workability. The improved durability performance was exhibited by thermally treated clay-based GPM specimens in terms of water absorption, sorptivity, drying shrinkage, abrasion and impact resistance. Thermally treated clay-based GPM showed better resistance towards chemical attack and revealed lower drying shrinkage. Hence based on the experimental investigation, it can be concluded that the clay (with and without thermal treatment) based GPM can be utilized in developing non-load bearing members for construction.

## 5. References


[1] Liew YM, Heah CY, Mustafa MAB, Kamarudin H. Structure and properties of clay-based geopolymer cements: a review. Prog Mater Sci. 2016;83:595-629.

[2] Duxson P, Provis JL, Lukey GC, Deventer JSJ. The role of inorganic polymer technology in the development of ‘green concrete’. Cem Concr Res. 2007;37(12):1590-1597.

[3] Li Z, Ding Z, Zhang Y. Development of sustainable cementitious materials. Proc Int Work Sustain Dev Concr Technol. 2004;1(1):55-76.

[4] Chindaprasirt P, Chareerat T, Hatanaka S, Cao T. High-strength geopolymer using fine high-calcium fly ash. J Mater Civ Eng. 2011;23(3):264-270.

[5] Saranya P, Nagarajan P, Shashikala AP. Performance studies on steel fiber–reinforced GGBS-dolomite geopolymer concrete. J Mater Civ Eng. 2021;33(2):04020447.

[6] Saranya P, Nagarajan P, Shashikala AP. Development of ground-granulated blast-furnace slag-dolomite geopolymer concrete. ACI Mater J. 2019;116(6):235-243.

[7] Paija N, Kolay PK, Mohanty M, Kumar S. Ground bottom ash application for conventional mortar and geopolymer paste. J Hazard Toxic Radioact Waste. 2020;24(1):04019025.

[8] Salih MA, Farzadnia N, Abang Ali AA, Demirboga R. Development of high strength alkali activated binder using palm oil fuel ash and GGBS at ambient temperature. Constr Build Mater. 2015;93:289-300.

[9] López MC, Araiza RJL, Ramírez MA, Avalos RJC, Bueno PJJ, Villareal MMS, et al. Synthesis and characterization of a concrete based on metakaolin geopolymer. Inorg Mater. 2009;45(12):1429-1432.

[10] Mehta A, Siddique R. Sustainable geopolymer concrete using ground granulated blast furnace slag and rice husk ash: strength and permeability properties. J Clean Prod. 2018;205:49-57.

[11] Laxman A, Sairam V, Srinivasan K, Muruganandam L. Synthesis and characterization of geopolymer from metakaolin and sugarcane bagasse ash. Constr Build Mater. 2020;258:119231.

[12] Fahim Huseien G, Mirza J, Ismail M, Ghoshal SK, Hussein AA. Geopolymer mortars as sustainable repair material: a comprehensive review. Renew Sustain Energy Rev. 2017;80:54-74.

[13] Priyadharshini P, Ramamurthy K, Robinson RG. Excavated soil waste as fine aggregate in fly ash based geopolymer mortar. Appl Clay Sci. 2017;146:81-91.

[14] Lekshmi S, Sudhakumar J. Engineering and durability performances of fly ash based geopolymer mortar containing aluminosilicate rich flood soil waste with and without lime treatment. Silicon. 2021;14(2):6141-6156.

[15] Ogundiran MB, Kumar S. Synthesis of fly ash-calcined clay geopolymers: reactivity, mechanical strength, structural and microstructural characteristics. Constr Build Mater. 2016;125:450-457.

[16] Zreig AMM, Akhras ANM, Attom MF. Influence of heat treatment on the behaviour of clayey soils. Appl Clay Sci. 2001;20:129-135.

[17] ASTM International. Standard specification for coal fly ash and raw or calcined natural pozzolan for use, https://www.astm.org/c0618-22.html [accessed 13 Febuary 2021].

[18] Zolfagharnasab A, Ramezanianpour AA, Zadeh BF. Investigating the potential of low grade calcined clays to produce durable LC3 binders against chloride ions attack. Constr Build Mater. 2021;303(12):124541.

[19] Chandrashekhar S, Ramaswamy S. Influence of mineral impurities on the properties of kaolin and its thermally treated products. Appl Clay Sci. 2002;21(3-4):133-142.

[20] Attah IC, Etim RK. Experimental investigation on the effects of elevated temperature on geotechnical behaviour of tropical resudial soils. SN Appl Sci. 2020;2(3):370.

[21] ASTM International. Standard test methods for sampling and testing fly ash or natural pozzolans for use in portland-cement concrete, https://www.astm.org/c0311-04.html [accessed 13 Febuary 2021].

[22] ASTM International. Standard test method for flow of hydraulic cement mortar, https://www.astm.org/c1437-20.html [accessed 13 Febuary 2021].

[23] ASTM International. Standard test method for compressive strength of hydraulic cement mortars (using 2-in. or [50-mm] cube specimens), https://www.astm.org/c0109_c0109m-01.html [accessed 13 Febuary 2021].

[24] ASTM International. Standard test method for rate of water absorption of masonry mortars, https://www.astm.org/c1403-15.html [accessed 13 Febuary 2021].

[25] ASTM International. Standard test method for measurement of rate of absorption of water by hydraulic cement concretes, https://www.astm.org/c1585-13.html [accessed 13 Febuary 2021].

[26] ASTM International. Standard test methods for determining the chemical resistance of concrete products to acid attack, https://www.astm.org/c1898-20.html [accessed 13 Febuary 2021].

[27] ASTM International. Standard test methods for chemical resistance of mortars, grouts, and monolithic surfacings and polymer concretes, https://www.astm.org/c0267-20.html.20.html [accessed 13 Febuary 2021].

[28] Flooring, Wall Finishing and Roofing Sectional Committee. Indian standard precast concrete block for paving-specification. 1st ed. New Delhi: Bureau of Indian Standards; 2006.

[29] ASTM International. Standard test method for length change of hardened hydraulic-cement mortar and concrete, https://www.astm.org/c0157_c0157m-08.html [accessed 13 Febuary 2021].

[30] ACI Committee 544. Measurement of properties of fiber reinforced concrete. Washington: American Concrete Institute; 1984. Report No.: ACI 544.2R-89.

[31] Zivica V, Palou M. Influence of heat treatment on the pore structure of some clays-precursors for geopolymer synthesis. Precedia Eng. 2016;151:141-148.

[32] Ogundiran MB, Ikotun OJ. Investigating the suitability of nigerian calcined kaolins as raw materials for geopolymer binders. Trans Indian Ceram Soc. 2014;73(2):138-142.

[33] Görhan G, Kürklü G. The influence of the NaOH solution on the properties of the fly ash-based geopolymer mortar cured at different temperatures. Compos Part B Eng. 2014;58:371-377.

[34] Dietel J, Warr LN, Bertmer M, Steudel A, Grathoff GH, Emmerich K. The importance of specific surface area in the geopolymerization of heated illitic clay. Appl Clay Sci. 2017;139:99-107.

[35] Ogundiran MB, Kumar S. Synthesis and characterisation of geopolymer from Nigerian clay. Appl Clay Sci. 2015;108:173-181.

[36] Nyamangara J, Munotengwa S, Nyamugafata P, Nyamadzawo G. The effect of hydroxide solutions on the structural stability and saturated hydraulic conductivity of four tropical soils. South Afr J Plant Soil. 2007;24(1):1-7.
[37] Yip CK, Lukey GC, Deventer JSJ. The coexistence of geopolymeric gel and calcium silicate hydrate at the early stage of alkaline activation. Cem Concr Res. 2005;35(9):1688-1697.
[38] Guo L, Wu Y, Xu F, Song X, Ye J, Duan P, et al. Sulfate resistance of hybrid fiber reinforced metakaolin geopolymer composites. Compos Part B Eng. 2020;183:107689.
[39] Niu X, Li Q, Hu Y, Tan Y, Liu C. Properties of cement based materials incorporating nano-clay and calcined nano-clay: a review. 2021;284:122820.
[40] Ramujee K, Potharaju M. Abrasion resistance of geopolymer composites. Procedia Mater Sci. 2014;6:1961-1966.
[41] Parathi S, Naagarajan P, Pallikkara SA. Ecofriendly 826 geopolymer concrete: a comprehensive review. J Clean Prod. 2021;23:1701-1713.
[42] Guo L, Wu Y, Xu F, Song X, Ye J, Duan P, et al. Sulfate resistance of hybrid fiber reinforced metakaolin geopolymer composites. Compos Part B Eng. 2020;183:107689.
[43] Jin M, Zheng Z, Sun Y, Chen L, Jin Z. Resistance of metakaolin-MSWI fly ash based geopolymer to acid and alkaline environments. J Non Cryst Solids. 2016;450:116-122.
[44] Saranya P, Naagarajan P, Shashikala AP. Engineering and durability properties of slag-dolomite geopolymer mortars. Proc Inst Civ Eng Constr Mater. 2020:1-12.
[45] Mermerdas K, Manguri S, Nassani DE, Oleiwi SM. Effect of aggregate properties on the mechanical and absorption characteristics of geopolymer mortar. Eng Sci Technol An int J. 2017;20(6):1642-1652.